



Published in final edited form as:

*J Plant Res.* 2014 November ; 127(6): 721–730. doi:10.1007/s10265-014-0654-y.

## New and unusual forms of calcium oxalate raphide crystals in the plant kingdom

**Vijayasankar Raman,**

National Center for Natural Products Research, School of Pharmacy, University of Mississippi, University, MS 38677, USA

**Harry T. Horner,** and

Department of Genetics, Development and Cell Biology and Microscopy and Nanolmaging Facility, Iowa State University, Ames, Iowa 50011-1020, USA

**Ikhlas A. Khan**

National Center for Natural Products Research, School of Pharmacy, University of Mississippi, University, MS 38677, USA

Department of Pharmacognosy, School of Pharmacy, University of Mississippi, University, MS 38677, USA

Department of Pharmacognosy, College of Pharmacy, King Saud University, Riyadh, Saudi Arabia

### Abstract

Calcium oxalate crystals in higher plants occur in five major forms namely raphides, styloids, prisms, druses and crystal sand. The form, shape and occurrence of calcium oxalate crystals in plants are species- and tissue-specific, hence the presence or absence of a particular type of crystal can be used as a taxonomic character. So far, four different types of needle-like raphide crystals have been reported in plants. The present work describes two new and unusual forms of raphide crystals from the tubers of *Dioscorea polystachya*—six-sided needles with pointed ends (Type V) and four-sided needles with beveled ends (Type VI). Both of these new types of needles are distinct from the other four types by each having a surrounding membrane that envelopes a bundle of 10–20 closely packed thin crystalline sheets. The previously known four types of needles have solid or homogenous crystalline material, surrounded by a membrane or lamellate sheath called a crystal chamber. Only the Type VI crystals have beveled ends and the needles of the other five types have pointed ends.

### Keywords

Anatomy; Calcium oxalate crystals; *Dioscorea polystachya*; Light microscopy; Raphides; Scanning electron microscopy; Yams

## Introduction

Inorganic calcium oxalate crystals are common in plants. They occur in different forms and shapes and are found in almost all major taxonomic groups of plants (Franceschi and Nakata 2005). Crystals have been observed in members of more than 215 plant families (McNair 1932) and occur in about 74 % of angiosperm families (Zindler-Frank 1976). The crystals are found in almost all organs of plants and in almost all types of tissues (Horner and Wagner 1995; Horner et al. 2012). The crystalline form can make up from about 1 % to over 90 % of a plant's dry mass (Braissant et al. 2004; Horner and Wagner 1995; Nakata 2003; Zindler-Frank 1976; 1987).

The primary role of calcium oxalate crystals may vary depending on the plant, organ and tissue in which they occur and can be characterized as: defense against herbivory, tissue support, calcium regulation and as an internal reservoir for calcium, ion balance, removal of toxic oxalic acid and gathering and reflection of light (Franceschi and Horner 1980; Franceschi and Nakata 2005; Nakata 2003). The formation of calcium oxalate crystals is genetically controlled and the crystals are usually formed in a defined shape and spatial location (Franceschi and Nakata 2005; Kausch and Horner 1982). Morphologically, the crystals are classified into five major forms: crystal sand, raphide, druse, styloid and prismatic (Franceschi and Horner 1980; Franceschi and Nakata 2005; Horner and Wagner 1995) and each category of crystal may show variations in its shape and size. Studies of the types of crystals and their macropatterns are species and genus specific and may contribute to understanding phylogenetic relationships (Horner et al. 2012; Lersten and Horner 2000; 2011; Prychid and Rudall 1999). The formation of calcium oxalate crystals in plants is not yet fully understood. Several studies have been conducted with the aim of filling this gap. Horner et al. (2000) showed the pathway of oxalate biosynthesis utilizes ascorbate as the primary precursor, and Nakata (2003) found that the ascorbate utilized is produced directly within the crystal idioblast itself. Plant crystals are formed from endogenously synthesized oxalic acid, which combines with calcium from the environment (Franceschi and Nakata 2005). Other subcellular features that influence crystal formation include changes in nuclear DNA (Kausch and Horner 1984b), an abundance of endoplasmic reticulum, acidic proteins, cytoskeletal components, and an intravacuolar matrix and organic paracrystalline bodies (Horner and Wagner 1995; Horner and Whitmoyer 1972; Nakata 2003).

Needle-shaped crystals called raphides typically occur in large numbers as closely packed bundles in tissues from green algae to flowering plants. They form in crystal membrane chambers within the vacuoles in specialized cells sometimes called crystal idioblasts (Arnott and Pautard 1970; Horner and Wagner 1995). The characteristic appearance, development and distribution of raphides, as well as other crystal shapes, have been used for taxonomic, pharmacognostic and toxicological purposes (Horner et al. 2012; Lampe and Fagerström 1968; Metcalfe and Chalk 1957; Sakai and Hanson 1974). Several studies have been conducted to elucidate the development and formation of raphides and raphide-containing idioblasts (Frey 1929; Horner and Whitmoyer 1972; Kausch and Horner 1983a; 1983b; 1984a; Mollenhauer and Larson 1966; Parameswaran and Schultze 1974; Sakai and Hanson 1974; Tilton and Horner 1980; Wattendorff 1976). Bruni et al. (1982) have described raphide formation as a complex process involving several cellular compartments. According to

Kostman and Franceschi (2000), raphide crystal idioblasts possess a cortical microtubule network that appears to limit an increase in cell diameter, but not elongation, resulting in the ellipsoidal shape of idioblasts.

The type of hydration of calcium oxalate influences the morphology of crystals. Two types of crystal forms, depending on the relative concentration of calcium and oxalate, are reported to occur in plants: (1) monohydrate (whewellite,  $\text{CaC}_2\text{O}_4 \cdot \text{H}_2\text{O}$ ; monoclinic crystal system) and (2) dihydrate (weddelite,  $\text{CaC}_2\text{O}_4 \cdot 2\text{H}_2\text{O}$ ; tetragonal crystal system) (Bouropoulos et al. 2001; Frey-Wyssling 1981; Horner and Wagner 1995). Some crystal shapes (i.e., druses, prisms) appear to have similar gross morphologies but are found to have both hydration states in plants (Arnott 1982; Franceschi and Horner 1980; Monje and Baran 2002). All reports to date indicate raphides are only whewellite.

In monocotyledons, three main types of calcium oxalate crystals, namely raphides, styloids and druses, are found; although intermediate forms are sometimes recorded (Prychid and Rudall 1999). Some of the monocot families (e.g. Iridaceae) are characterized by the presence of only styloids in most genera and they completely lack raphides (Goldblatt et al. 1984; Rudall 1994, 1995; Wu and Cutler 1985) while in some other families (e.g. Hypoxidaceae), raphides are present and styloids are absent. Therefore, the presence or absence of a particular type of calcium oxalate crystal can be used as a taxonomic character. However, both raphide and styloid crystals occur in many other families (Horner et al. 2012; Prychid and Rudall 1999; Svoma and Greilhuber 1988).

Within the order Dioscoreales, raphides are absent in Burmanniaceae and Nartheciaceae while they are present in Dioscoreaceae, Stenomeridaceae, Thismiaceae and Trichopodaceae (Ayensu 1972; Prychid and Rudall 1999). Okoli and Green (1987) have observed unusual tiny calcium oxalate crystals associated with starch grains in seven species of *Dioscorea*. According to Ayensu (1972), styloids are normally absent but rarely present in *Dioscorea*. Solitary crystals are present in *D. alata* (Al-Rais et al. 1971) and small crystals are found adjacent to vascular bundles in *D. minutiflora* (Prychid and Rudall 1999).

Styloid crystals (Greek: *stylos* = column/pillar), also known as pseudo-raphides, are usually longitudinally elongated forming rectangular columns. They tend to be solitary within a cell (Prychid and Rudall 1999). Several forms of styloids with varied shapes and sizes are reported in plants (Arnott 1981; Frey 1929; Kollbeck et al. 1914). Styloids may have pointed or squared ends and the ends in some crystals are roofed by two prisms (Frey-Wyssling 1981) giving a beveled shape to the tips. Styloid crystals are characteristic of some families of Asparagales including Agavaceae, Alliaceae, Convallariaceae, Asphodelaceae, Iridaceae and Xanthorrhoeaceae (Arnott et al. 1965; Prychid and Rudall 1999; Wattendorff 1976; 1978).

Raphide (Greek: *rhaphis* = needle) crystals are stacks of hundreds to thousands of bundled needles occurring usually in the vacuoles (Arnott and Pautard 1970; Franceschi and Nakata 2005). Raphide crystals are widely found in several families of angiosperms. They show high birefringence indicating that they are monohydrate. Wattendorff (1976) observed various crystal faces on these crystals in *Agave americana* and *Cordyline indivisa*. In

developing leaves, the growing raphides originally have rectangular cross sections, and when mature they may convert to being hexagonal or octagonal in cross sections. The six- to eight-sided middle of the needles becomes rectangular towards the tapering ends of mature needles. Frey-Wyssling (1981) opines that since *A. americana* contains both raphides and styloids, it is likely that the rectangular forms described by Wattendorff (1976) actually corresponds to the rectangular styloid, as is the case with the rectangular raphides in the rhizome of *Polygonatum multiflorum*.

Four types of needles (Fig. 1a) have been reported so far (Horner and Wagner 1995). They are represented by: *Psychotria* (Type I), *Lemna* (Type II), *Agave* (Type III) and *Vitis* (Type IV) types. Type I crystals are four-sided, square in cross-section, and pointed at ends. Type II crystals found in *Lemna* have four sides, appearing as a solid square in the middle but toward each end there are two opposing grooves giving a 'H' shape in cross section. Type III needles have six to eight sides, hexagonal or octagonal in cross section and pointed at both the ends. The Type IV crystals have four sides with a median division, pointed at one end and quiver-shaped at the other end.

In this study we present two new and unusual types of raphides found in the tissues of *Dioscorea* tubers.

## Materials and methods

Fresh tubers of *Dioscorea polystachya* Turcz. were collected from plants grown in the garden as well as greenhouse at the Maynard W. Quimby Medicinal Plant Garden (MPG) of the University of Mississippi, University, MS. Herbarium specimens (NCNPR # 13124) of the plants were prepared and deposited in the herbarium of MPG.

### Preparation of samples for light microscopy

Fresh tuber samples were fixed in formalin-acetic acid-alcohol (FAA) for two days and washed in distilled water. Free-hand sections of the tubers were made in various thicknesses at different angles using razor blades. The sections were mounted on glass slides in a drop of glycerin. The mounted sections were then analyzed and imaged using Nikon E600 and Nikon E600 POL microscopes equipped with Nikon DS-Fiv camera systems and Nikon Elements imaging software (Nikon Inc., Tokyo, Japan). Idioblasts containing bundles of raphide crystals were isolated from fresh sections using needles and forceps while observing them with a Nikon SMZ-U Stereomicroscope.

### Preparation of samples for scanning electron microscopy

Freshly collected tuber samples were sliced at various angles and the pieces were fixed overnight in 2.5 % glutaraldehyde in 0.2 M sodium phosphate buffer (pH 7.4) and washed in distilled water and dehydrated through increasing concentrations of ethanol (Hayat 2000). The dehydrated specimens were then dried in a Critical Point Dryer (Denton Vacuum, Moorestown, NJ, USA) using liquid CO<sub>2</sub>. The fully dried samples were then mounted on aluminum stubs using sticky carbon tabs and sputter coated with gold (Hummer 6.2 Sputter Coater, Anatech USA, Union City, CA, USA). Digital images of the specimens were captured using a JSM-5600 Scanning Electron Microscope (SEM) (JEOL USA Inc.,

Peabody, MA, USA). Some of the critical point dried samples were coated with platinum (15 nm) using an EMS 150T ES Sputter Coater (Electron Microscopy Sciences, Hatfield, PA, USA). These samples were then mounted on aluminum stubs, viewed, and imaged using a JEOL JSM-6500F Field Emission SEM. Elemental analyses were done with a Bruker Quantax 200 X Flash EDX Spectrometer System attached to a Zeiss EVO 50 Variable Pressure SEM at 10 kV, using INCA-Mapping software.

## Results

During the anatomical study (Raman et al. 2014) of various species of *Dioscorea* L. (Dioscoreaceae), two unusual types of raphide crystals were observed in the tubers of *D. polystachya*. A survey of the literature showed that they did not represent any of the four types (Fig. 1a) of raphides that were known to occur in the Plant Kingdom (Horner and Wagner 1995). Therefore, the two unusual crystal types are described here as Type V and Type VI (Fig. 1b). The composite needles in both of these types consist of plate-like sheets, occurring in bundles that are embedded in mucilage within crystal idioblast vacuoles. The unique feature of these raphide crystals is that they are lamellate, each containing 10–20 thin, compact crystalline sheets arranged parallel to the longitudinal axis of the needle, and enclosed by a membrane. The crystalline sheets are either free or partly fused.

The crystal units of Type V (Figs. 2, 3) are usually six-sided or rarely eight-sided (appearing more or less circular in light microscopy; Fig. 2c, d), pointed at both the ends (Fig. 2b, g–i), measuring 125–160  $\mu\text{m}$  long. Cross-sections at midpoint of the crystal are hexagonal (Fig. 2a–f) or octagonal, and narrowly elliptic (Fig. 2h) in outline near the ends. The crystals are 1.5–4.5  $\mu\text{m}$  across, with the sides measuring 0.9–2.0  $\mu\text{m}$  near middle point and gradually tapering towards the pointed ends. The number of crystal units in each bundle range from 140 to 250. The bundle, measuring 29–47  $\mu\text{m}$  in diameter, is embedded in thick mucilage within the crystal idioblast vacuoles (Fig. 2a, c, g). In sectional view, the compact crystal bundle with its six- to eight-sided crystal units displays a honeycomb-like structure (Fig. 3a, f). In some bundles, the crystal units are separated from each other and these spaces are filled with mucilage.

The crystal units of Type VI (Fig. 4a–i) are four-sided (Fig. 4b, c, g–i), with beveled ends (Fig. 4d, e), measuring 130–165  $\mu\text{m}$  long, occurring in bundles. The bundles are 59–65  $\mu\text{m}$  in diameter. Cross sections at midpoint of the crystal is square (Fig. 4b, c) or broadly rectangular (Fig. 4h, i), and narrowly rectangular near the beveled ends (Fig. 4g). The sides of the square-type crystals measure 2.4–3.3  $\mu\text{m}$ . The sides of the rectangular-shaped composite crystals measure 3.3–5.8  $\times$  2.4–3.4  $\mu\text{m}$  wide. The width of the beveled ends is almost equal to the width of the crystal. The crystal units of this type are usually loosely arranged in a bundle embedded in mucilage (Fig. 4a–e).

The crystal units in these two types of crystals contain a series of 10–20 thin crystalline sheets that together are enveloped by a single crystal membrane (Figs. 3a–i, 4f–i). The crystalline sheets are closely packed within the enveloping membrane and are arranged parallel to the length of the crystal unit (Figs. 3, 4f). In cross-sectional view, the single crystal membrane is hexagonal or rarely octagonal in outline in Type V and is rectangular or

square in Type VI composite crystals. In some crystals, the crystalline sheets are clearly separated (Fig. 3e, f) whereas in others they appear to be more or less fused (Figs. 3c, d, 4h, i).

The tubers of *Dioscorea polystachya* show three regions in cross section: a ring of cork, followed by a narrow band of cortex (the outer ground tissue) and the wide central cylinder (including the vascular bundles and the inner ground tissue). Cortical cells are devoid of starch whereas the cells of the inner ground tissue are filled with large amounts of starch grains. The tubers of this species are rich in various types of raphide crystals which are concentrated in the cortex region and sparingly distributed in the ground tissue (Raman et al. 2014). Type III (*Agave*) crystals (Fig. 3g–i) are abundant in the cortex as well as the ground tissue. Occasionally, Type IV (*Vitis*) crystals are also observed. Type V and Type VI crystals are uncommon in comparison to Type III in this species. Of the first two types, the Type V crystal is more common. The Type V crystal is usually found in the cortex (Fig. 2a, e, f) but it is also formed in the ground tissue. The Type VI crystal is observed only in the ground tissue (Fig. 4d, e). Raphide crystals are also present in the leaves of *D. polystachya*. While Type III crystals are most common, the new Type VI crystals are infrequently observed in the leaves.

### Energy-dispersive X-ray spectroscopy (EDS or EDX) microanalysis of crystals

Both Type V and Type VI crystals were analyzed for their elemental composition. Both types of crystals and their crystalline contents produced similar spectra showing prominent peaks for calcium (Ca), carbon (C) and oxygen (O). The peaks showed slight variations in different spectra and the spectrum in Fig. 5 is representative of all spectra of the two new types of crystals. The atomic ratio (1:2:4) of these three elements derived from the spectra indicated that the crystals were of calcium oxalate ( $\text{CaC}_2\text{O}_4$ ), and not  $\text{CaCO}_3$ ; also based on birefringence and crystal shape. The samples initially sputter coated with gold (Au) and platinum (Pt) showed peaks for these heavy metals. None of the spectra showed peaks for silicon, ruling out the possibility of the crystals being silica.

### Discussion

The finding of two new types of raphides (Types V and VI) is not surprising in that relatively few examples of raphides have been observed in fine detail within the Plant Kingdom. These observations raise a number of questions about the development of these crystals and the unique composition of many individual planar crystals making up a single raphide having two different morphological shapes and ends (Type V versus Type VI). They could be related to different hydration (mono- versus di-hydrate) forms of the calcium oxalate even though this has not been confirmed. This highly unusual condition of lamination to form a composite crystal is biologically and crystallographically perplexing.

The question of whether these two types of crystals may be artifacts or variants of existing types also need to be considered. Bright-field and polarized-light microscope views of fresh sections of the crystals do not clearly show the lamellated condition, perhaps due to the limitation in magnification and resolution. However, fractured specimens prepared for SEM clearly show the lamellated conditions as described above. Multiple preparations are

consistent in showing both the lamellated and solid raphides in separate idioblasts. The Type V crystal is morphologically similar to Type III so V can be a variant of III, but both the types differ in their anatomy: lamellated in Type V (Fig. 3a–f) and solid in Type III (Fig. 3g–i). Several studies focusing formation and development of crystals are available in the literature but none of them report the laminated nature of raphides. Also, there are no intermediary forms or different developmental stages reported in the literature to conclude Type V crystal as a variant of Type III. It is also not clear at this point whether the crystalline sheets fuse during the course of maturation to eventually form the solid needle. If this is true then the Type V will convert to the Type III. On the other hand, Type VI crystal is clearly different from the four previously reported types of raphides by having beveled ends, a feature found in styloid crystals, which usually occur as individual crystals in cells. For the question of whether this is also a variant, it is not known at this stage how the beveled ends would transform to points, since none of the other types of raphides have beveled ends. Noticeably, Type V and Type VI crystals have similar anatomy. For these reasons, we believe the Type V and Type VI raphides (*Dioscorea* types) described in this study represent two new raphide crystal types. Detailed studies focusing on the formation and development of these unusual as well as previously described types of raphide crystals would possibly provide new insights on the biogenesis of raphide needles and also help to understand their developmental stages and possible transformations in their morphology and anatomy.

## Acknowledgments

This study was supported by Grant Number P50AT006268 from the National Center for Complementary and Alternative Medicines (NCCAM), the Office of Dietary Supplements (ODS) and the National Cancer Institute (NCI), and by partial support from the United States Food and Drug Administration (FDA) Specific Cooperative Research Agreement number U01 FD004246-01. We thank Ahmed M. Galal and Amar Chittiboyina of National Center for Natural Products Research, University of Mississippi, MS for helpful suggestions; and Rooban Thirumalai and Amanda Lawrence of Institute for Imaging and Analytical Technologies (I<sup>2</sup>AT), Mississippi State University, MS for help in FE-SEM imaging and elemental analysis.

## References

- Al-Rais AH, Myers A, Watson L. Isolation and properties of oxalate crystals from plants. *Ann Bot Lond.* 1971; 35:1213–1218.
- Arnott HJ. An SEM [scanning electron microscopy] study of twinning in calcium oxalate crystals of plants [*Diospyros virginiana*]. *Scan Electron Micros.* 1981; 1981:225–234.
- Arnott, HJ. Three systems of biomineralization in plants with comments on the associated organic matrix. In: Nancollas, GH., editor. *Biological mineralization and demineralization*. Springer; Berlin: 1982. p. 199-218.
- Arnott, HJ., Pautard, FGE. Calcification in plants. In: Schraer, H., editor. *Biological calcification: cellular and molecular aspects*. Springer; New York: 1970. p. 375-446.
- Arnott HJ, Pautard FGE, Steinfink H. Structure of calcium oxalate monohydrate. *Nature.* 1965; 208:1197–1198.
- Ayensu, ES. *Anatomy of the monocotyledons: VI. Dioscoreales*. Clarendon Press; Oxford: 1972.
- Bouropoulos N, Weiner S, Addadi L. Calcium oxalate crystals in tomato and tobacco plants: morphology and in vitro interactions of crystal-associated macromolecules. *Chem Eur J.* 2001; 7:1881–1888. [PubMed: 11405466]
- Braissant O, Cailleau G, Aragno M, Verrecchia EP. Biologically induced mineralization in the tree *Milicia excelsa* (Moraceae): its causes and consequences to the environment. *Geobiology.* 2004; 2:59–66.

- Bruni A, Dall'Olio G, Tosi B. A study of the development of raphide-forming cells in *Musa paradisiaca* using fluorescence microscopy. *New Phytol.* 1982; 92:581–587.
- Crowther, A. Reviewing raphides: issues with the identification and interpretation of calcium oxalate crystals in microfossil assemblages. In: Fairbairn, A.O'Connor, S., Marwick, B., editors. *New Directions in Archaeological Science*. ANU E-Press; Canberra: 2009. p. 105–118. *Terra Australis*, vol 28
- Franceschi VR, Horner HT. Calcium oxalate crystals in plants. *Bot Rev.* 1980; 46:361–427.
- Franceschi VR, Nakata PA. Calcium oxalate in plants: formation and function. *Annu Rev Plant Biol.* 2005; 56:41–71. [PubMed: 15862089]
- Frey A. Calciumoxalat-monohydrat und trihydrat in der Pflanze. Eine physiologische Studie auf Grund der Phasenlehre. *Vierteljahrsschr Naturf Ges Zurich.* 1929; 70:1–65.
- Frey-Wyssling A. Crystallography of the two hydrates of crystalline calcium oxalate in plants. *Am J Bot.* 1981; 68:130–141.
- Goldblatt P, Henrich JE, Rudall P. Occurrence of crystals in Iridaceae and allied families and their phylogenetic significance. *Ann Mo Bot Gard.* 1984; 71:1013–1020.
- Hayat, MA. *Principles and techniques of electron microscopy: biological applications*. Cambridge University Press; New York: 2000.
- Horner, HT., Wagner, BL. Calcium oxalate formation in higher plants. In: Khan, SR., editor. *Calcium oxalate in biological systems*. CRC Press; Boca Raton: 1995. p. 53–72.
- Horner HT, Whitmoyer RE. Raphide crystal cell development in leaves of *Psychotria punctata* (Rubiaceae). *J Cell Sci.* 1972; 11:339–355. [PubMed: 4342516]
- Horner HT, Kausch AP, Wagner BL. Ascorbic acid: a precursor of oxalate in crystal idioblasts of *Yucca torreyi* in liquid root culture. *Int J Plant Sci.* 2000; 161:861–868.
- Horner HT, Wanke S, Samain MS. A comparison of leaf crystal macropatterns in the two sister genera *Piper* and *Peperomia* (Piperaceae). *Am J Bot.* 2012; 99:983–997. [PubMed: 22623612]
- Kausch AP, Horner HT. A comparison of calcium oxalate crystals isolated from callus cultures and their explant sources. *Scan Electron Micros.* 1982; I:199–211.
- Kausch AP, Horner HT. The development of mucilaginous raphide crystal idioblasts in young leaves of *Typha angustifolia* L. (Typhaceae). *Am J Bot.* 1983a; 70:691–705.
- Kausch AP, Horner HT. Development of syncytial raphide crystal idioblasts in the cortex of adventitious roots of *Vanilla planifolia* L. (Orchidiaceae). *Scan Electron Micros.* 1983b; II:893–903.
- Kausch AP, Horner HT. Differentiation of raphide crystal idioblasts in isolated root cultures of *Yucca torreyi* (Agavaceae). *Can J Bot.* 1984a; 62:1474–1484.
- Kausch AP, Horner HT. Increased nuclear DNA content in raphide crystal idioblasts during development in *Vanilla planifolia* L. (Orchidaceae). *Eur J Cell Biol.* 1984b; 33:7–12. [PubMed: 6698045]
- Kollbeck F, Goldschmidt V, Schroder R. Ueber Whewellit. *Beitr Kristallogr Miner.* 1914; 1:1914–1918.
- Kostman TA, Franceschi VR. Cell and calcium oxalate crystal growth is coordinated to achieve high-capacity calcium regulation in plants. *Protoplasma.* 2000; 214:166–179.
- Lampe, KF., Fagerström, R. *Plant toxicity and dermatitis: a manual for physicians*. Williams & Wilkins; Baltimore: 1968.
- Lersten NR, Horner HT. Calcium oxalate crystal types and trends in their distribution patterns in leaves of *Prunus* (Rosaceae: Prunoideae). *Plant Syst Evol.* 2000; 224:83–96.
- Lersten NR, Horner HT. Unique calcium oxalate “duplex” and “concretion” idioblasts in leaves of tribe Naucleaeae (Rubiaceae). *Am J Bot.* 2011; 98:1–11. [PubMed: 21613079]
- McNair JB. The intersection between substances in plants: essential oils and resins, cyanogen and oxalate. *Am J Bot.* 1932; 19:255–271.
- Metcalfe, CR., Chalk, L. *Anatomy of the dicotyledons*. Clarendon Press; Oxford: 1957.
- Mollenhauer H, Larson D. Developmental changes in raphide-forming cells of *Vanilla planifolia* and *Monstera deliciosa*. *J Ultrastruct Res.* 1966; 16:55–70. [PubMed: 5956757]



- Monje PV, Baran EJ. Characterization of calcium oxalates generated as biominerals in cacti. *Plant Physiol.* 2002; 128:707–713. [PubMed: 11842173]
- Nakata PA. Advances in our understanding of calcium oxalate crystal formation and function in plants. *Plant Sci.* 2003; 164:901–909.
- Okoli BE, Green BO. Histochemical localization of calcium oxalate crystals in starch grains of yams (*Dioscorea*). *Ann Bot Lond.* 1987; 60:391–394.
- Parameswaran N, Schultze R. Fine structure of chambered crystalliferous cells in the bark of *Acacia senegal*. *Z Pflanzenphysiol.* 1974; 71:90–93.
- Prychid CJ, Rudall PJ. Calcium oxalate crystals in monocotyledons: a review of their structure and systematics. *Ann Bot Lond.* 1999; 84:725–739.
- Raman V, Galal AM, Avula B, Sagi S, Smillie TJ, Khan IA. Application of anatomy and HPTLC in characterizing species of *Dioscorea* (Dioscoreaceae). *J Nat Med.* 2014; doi: 10.1007/s11418-014-0849-5
- Rudall P. Anatomy and systematics of Iridaceae. *Bot J Linn Soc.* 1994; 114:1–21.
- Rudall, P. Iridaceae. In: Cutler, DF., Gregory, M., editors. *Anatomy of the monocotyledons*. Vol. VIII. Oxford University Press; Oxford: 1995.
- Sakai WS, Hanson M. Mature raphid and raphid idioblast structure in plants of the edible aroid genera *Colocasia*, *Alocasia*, and *Xanthosoma*. *Ann Bot Lond.* 1974; 38:739–748.
- Svoma E, Greilhuber J. Studies on systematic embryology in *Scilla* (Hyacinthaceae). *Plant Syst Evol.* 1988; 161:169–181.
- Tilton VR, Horner HT. Calcium oxalate raphide crystals and crystalliferous idioblasts in the carpels of *Ornithogalum caudatum*. *Ann Bot Lond.* 1980; 46:533–539.
- Wattendorff J. A third type of raphide crystal in the plant kingdom: six-sided raphides with laminated sheaths in *Agave americana* L. *Planta.* 1976; 130:303–311. [PubMed: 24424644]
- Wattendorff J. Ultrastructure and development of the calcium oxalate crystal cells with suberin-like crystal sheaths in the bark and secondary xylem of *Acacia senegal* Willd. *Protoplasma.* 1978; 95:193–206.
- Wu QG, Cutler D. Taxonomic, evolutionary and ecological implications of the leaf anatomy of rhizomatous *Iris* species. *Bot J Linn Soc.* 1985; 90:253–303.
- Zindler-Frank E. Oxalate biosynthesis in relation to photosynthetic pathway and plant productivity—a survey. *Z Pflanzenphysiol.* 1976; 80:1–13.
- Zindler-Frank, E. Calcium oxalate crystals in legumes. In: Stirton, E., editor. *Advances in legume systematics*, part 3. Royal Botanic Gardens; Kew: 1987. p. 279-316.

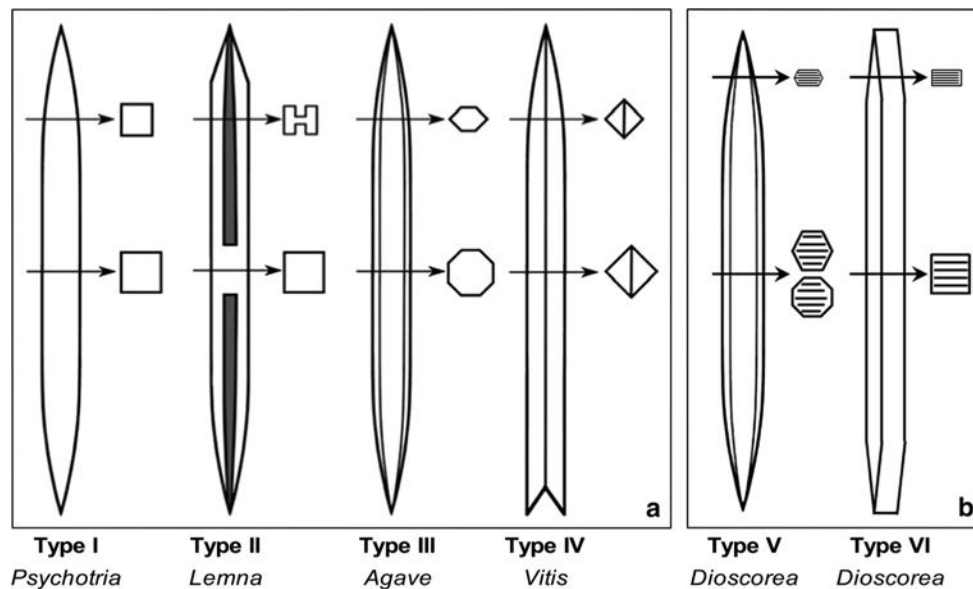


**Fig. 1.** Types of raphide crystals. **a** diagrams of four known shapes of plant raphide crystals (Types I to IV) showing longitudinal and cross-sectional views [adopted from Crowther (2009)—originally redrawn from Horner and Wagner (1995)]. **b** Two shapes (Types V and VI) of raphide crystals described in this study from *Dioscorea polystachya* tuber showing their morphology and cross-sections. Note the crystalline sheets as seen in cross-sections; and beveled end forms in Type VI crystal

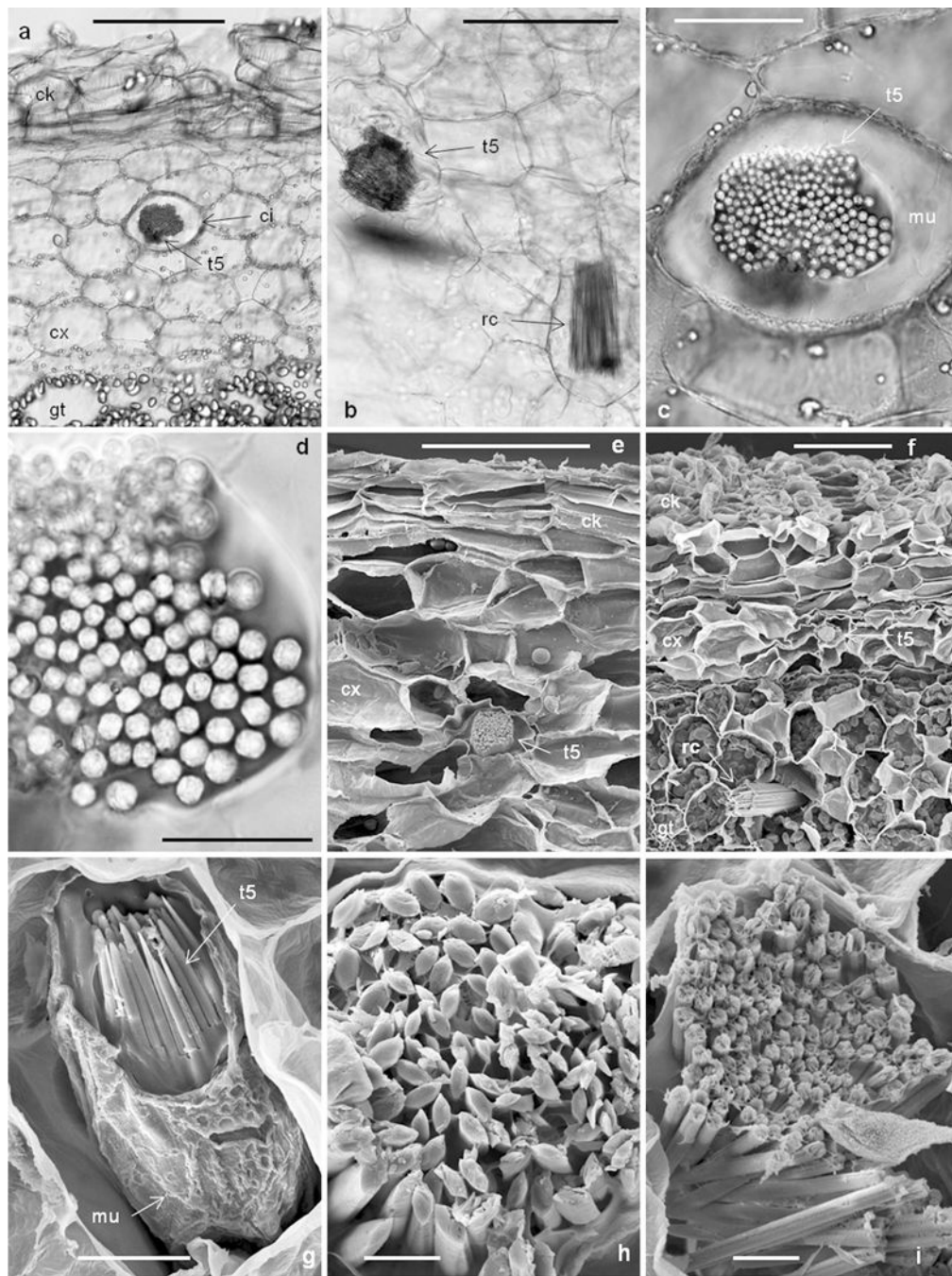


**Fig. 2.** Type V raphide crystals in *Dioscorea polystachya* tuber. **a–d** Light microscopy (LM), free-hand sections, unstained; **e–i** SEM. **a** Portion of tuber in transection (TS) showing a crystal idioblast in cortex containing Type V crystal bundle. **b** Portion of cortex showing Type V crystal and a usual Type III raphide bundle. **c, d** TS of a Type V crystal idioblast in cortex—bundle of needles is embedded in thick mucilage. **e** Portion of tuber in TS showing a Type V bundle in cortex. **f** Type V bundle in cortex and an usual Type III bundle in ground tissue. **g** View of a Type V raphide bundle embedded in mucilage. **h** TS of Type V crystal near

pointed end. **i** Fractures of Type V crystal showing sectional and side views and pointed ends. *ci* crystal idioblast, *ck* cork, *cx* cortex, *gt* ground tissue, *mu* mucilage, *rc* usual Type III raphide crystals, *sg* starch grains, *t5* Type V crystals. Bars 200  $\mu\text{m}$  (**a, b, e, f**), 50  $\mu\text{m}$  (**c**), 20  $\mu\text{m}$ , (**d, g**), and 10  $\mu\text{m}$  (**h, i**)

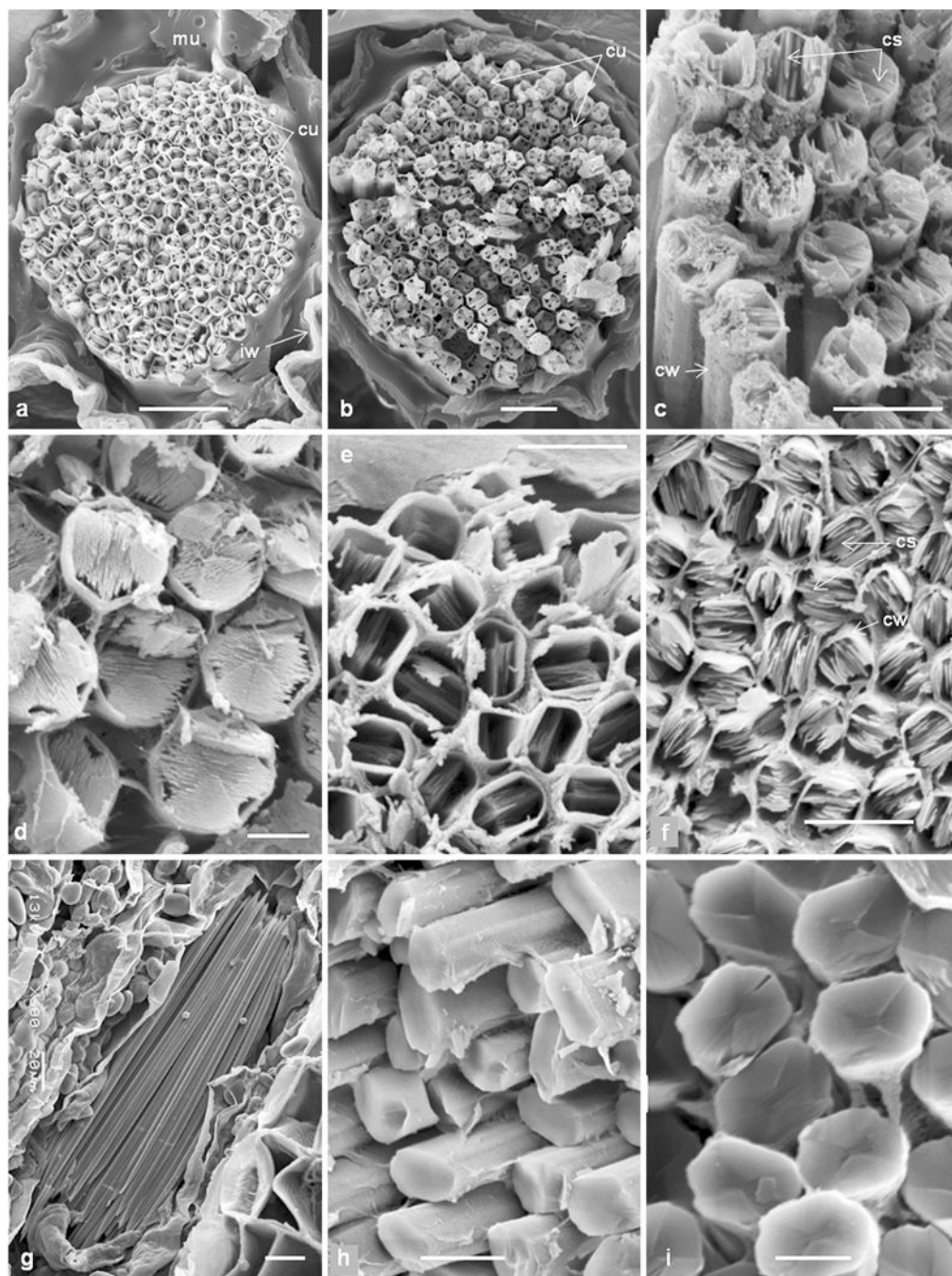


**Fig. 3.** SEM images of Type V and Type III raphide crystal bundles in *Dioscorea polystachya* tuber. **a–f** Type V bundles. Each Type V bundle consists of 140–250 needles or crystal units within crystal idioblast and bundle is embedded in thick mucilage. Each crystal unit/needle consists of 10–20 compactly packed thin crystalline sheets enclosed by a six- or eight-sided membrane. **g–i** Type III bundles. **g** Entire view of Type III raphide crystals showing pointed ends. **h, i** TS of Type III crystals showing solid cut faces. *cs* crystalline sheets, *cu* crystal

units, *cw* crystal unit wall, *iw* idioblast cell wall, *mu* mucilage. *Bars* 10  $\mu\text{m}$  (**a**), 5  $\mu\text{m}$  (**b**, **c**, **e**, **f**, **h**), 2  $\mu\text{m}$  (**d**, **i**), and 20  $\mu\text{m}$  (**g**)

Author Manuscript

Author Manuscript

Author Manuscript

Author Manuscript

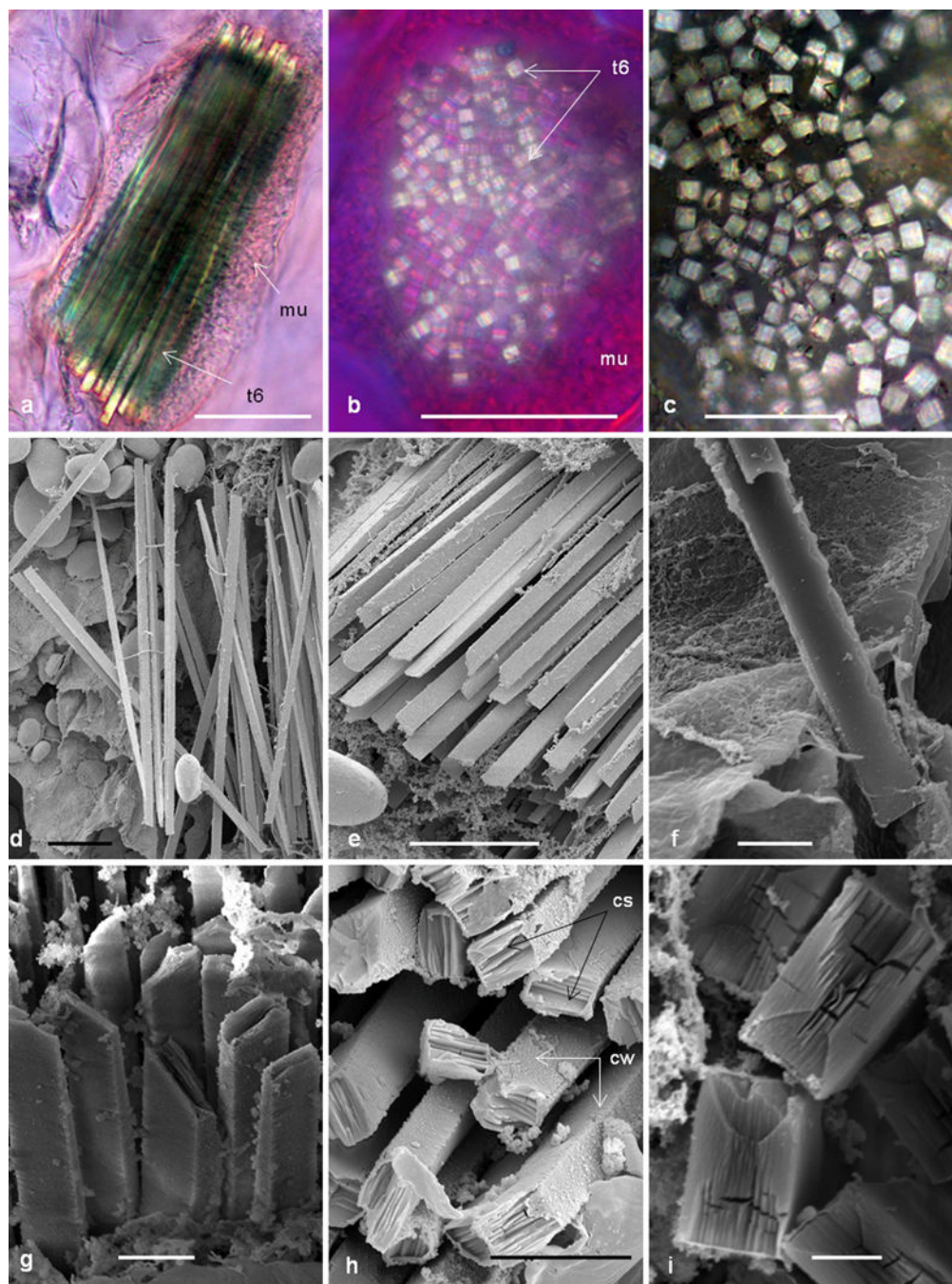


**Fig. 4.** Type VI raphide crystals in *Dioscorea polystachya* tuber. **a, b** Polarized light. **c** LM. **d–i** SEM. **a** An isolated bundle of Type VI crystals. **b, c** In transection (TS) of Type VI raphide crystals showing four-sided crystal units/needles. **d** Entire view of individual crystals of Type VI. **e** A portion of bundle showing beveled ends of needles. **f** A longitudinal fracture showing inner view of needle. **g** TS of crystals near tip/end of crystal is narrowly rectangular in outline. **h, i** TS at the mid-portion of Type VI crystal has four sides and rectangular in

outline. *cs* crystalline sheets, *cw* crystal unit wall, *mu* mucilage, *t6* Type VI crystals. *Bars* 50  $\mu\text{m}$  (**a, b**), 20  $\mu\text{m}$  (**c–e**), 5  $\mu\text{m}$  (**f–h**), and 2  $\mu\text{m}$  (**i**)

Author Manuscript

Author Manuscript

Author Manuscript

Author Manuscript



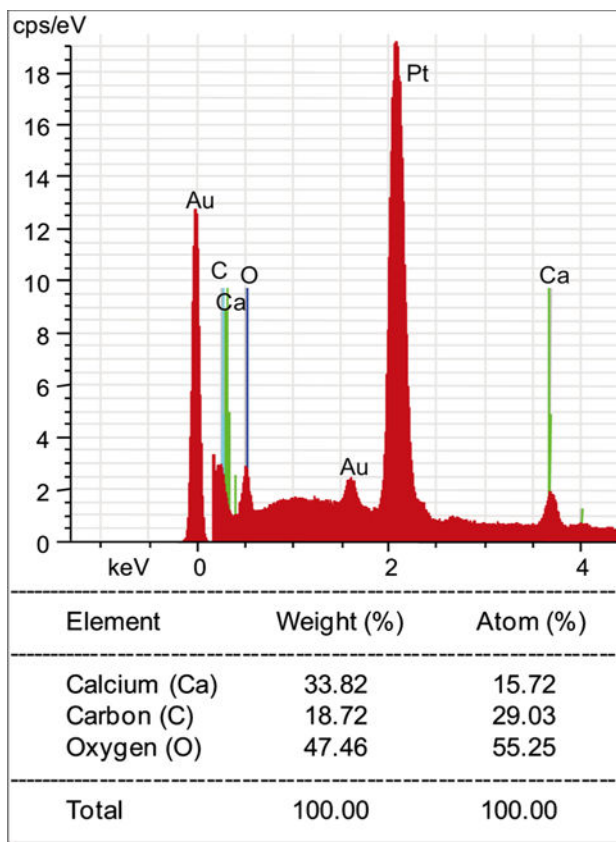


**Fig. 5.** SEM X-ray energy dispersive elemental analysis of isolated Type V and Type VI raphide crystals. Crystals were coated with gold (Au) and platinum (Pt). Remaining *peaks* of C, Ca and O indicate both crystal types are composed of calcium oxalate ( $\text{CaC}_2\text{O}_4$ )